

# RSC Advances



This is an *Accepted Manuscript*, which has been through the Royal Society of Chemistry peer review process and has been accepted for publication.

*Accepted Manuscripts* are published online shortly after acceptance, before technical editing, formatting and proof reading. Using this free service, authors can make their results available to the community, in citable form, before we publish the edited article. This *Accepted Manuscript* will be replaced by the edited, formatted and paginated article as soon as this is available.

You can find more information about *Accepted Manuscripts* in the [Information for Authors](#).

Please note that technical editing may introduce minor changes to the text and/or graphics, which may alter content. The journal's standard [Terms & Conditions](#) and the [Ethical guidelines](#) still apply. In no event shall the Royal Society of Chemistry be held responsible for any errors or omissions in this *Accepted Manuscript* or any consequences arising from the use of any information it contains.

## ARTICLE

## A novel coumarin derivative as sensitive probe for tracing intracellular pH changes

Cite this: DOI: 10.1039/x0xx00000x

Mengqiang Liu<sup>a</sup>, Minshan Hu<sup>c</sup>, Qian Jiang<sup>a</sup>, Zhiyun Lu<sup>a</sup>, Yan Huang<sup>a</sup>, Yanfei Tan<sup>\*b</sup>, Qing Jiang<sup>\*a,b</sup>

Received 00th January 2012,  
Accepted 00th January 2012

DOI: 10.1039/x0xx00000x

[www.rsc.org/](http://www.rsc.org/)

A new pH sensitive probe, 7-diethylamino-3-[2-(4-piperidin-1-yl-phenyl)-vinyl]-chromen-2-one (**CS-P**), was designed and synthesized. This probe was constructed by introduction of piperidine to the coumarin stem. It exhibited high pH sensitive ranged from pH 5.9 to pH 3.0 ( $pK_a = 4.55$ ), *in vitro* cell imaging showed that its fluorescence intensity was distinctly related to the cellular pH changes induced by chloroquine or dexamethasone. Demonstrated with good cell membrane permeability and high pH sensitivity, this probe is suitable for tracing the intracellular pH changes from neutral to acidic conditions.

### Introduction

Intracellular pH plays key roles in modulating cell growth and differentiation, enzyme and tissue functions, such as cell cycle control,<sup>1</sup> cellular proliferation and apoptosis,<sup>2</sup> membrane potential and ion regulation,<sup>3</sup> muscle contraction<sup>4</sup> and multidrug resistance (MDR).<sup>5</sup>

Abnormal pH values are associated with inappropriate cell functions, growth, and division, which can cause many serious human diseases. An enhanced activity of Na(+)/Li(+) countertransport, studied as a surrogate of Na(+)/H(+) exchanger, has been described in red blood cells of patients with cardiac syndrome X.<sup>6</sup> Mucopolipidosis type IV (MLIV) is a neurodegenerative channelopathy and in MLIV the lysosomal pH is lower than normal.<sup>7</sup> Eukaryotic cell contains some compartments with different acidity degrees, for example, the cytoplasm is slightly alkaline at about pH 7.2, whereas some organelles, such as lysosomes and endosomes, have intracompartamental pHs of 4.0-6.0.<sup>8</sup> Lysosomes and endosomes which participate in the critical functions of endocytic and digestive processes have pH value of 4.7 and 5.5, respectively.<sup>9</sup> Therefore, monitoring of pH changes in live cells is critical for studying cellular functions and further understanding physiological and pathological processes.

There are many popular techniques to measure intracellular pH, including microelectrodes, nuclear magnetic resonance (NMR), and molecular spectroscopy. Among these techniques, fluorescence spectroscopy has attracted much more attention due to its excellent sensitivity, fast response time, high signal-to-noise ratio and the ability to continuously monitor the rapid kinetic pH changes.<sup>10</sup>

Fluorescent probe offers a unique approach for visualizing morphological details of tissues with subcellular resolution and has become a powerful tool for manipulating and investigating living cells and even animals.<sup>11-14</sup> There are different kinds of fluorescent probes with various skeleton structure, including rhodamine,<sup>15</sup> BODIPY,<sup>16</sup> fluorescein,<sup>17</sup> tricarboyanine,<sup>18</sup> benzo[a]phenoxazine,<sup>19</sup> coumarin<sup>20</sup> etc. From these fluorophores, some special probes with pH sensitivity can be designed and synthesized by changing functional groups to these skeletons.

Coumarins are a group of good candidates, because they have very high fluorescence quantum yield,<sup>21</sup> large Stokes shift,<sup>22</sup> excellent light stability, and low toxicity.<sup>23</sup> At the same time, coumarin derivatives have expanded emission profiles tunable from the blue to near-infrared (NIR) region by simply changing donors at either the 6- or 7-position and the electron acceptor at either 3- or 4- position of the coumarin core structure.<sup>24</sup> So far, based on the coumarin platform, a number of pH sensitive fluorescent probes with different functional groups had been constructed.<sup>25-27</sup> However, connecting H<sup>+</sup> binding sites to the coumarin skeleton by styrene bond for increasing conjugated system it has not been reported.

In this paper we developed a new coumarin derivative, termed 7-diethylamino-3-[2-(4-piperidin-1-yl-phenyl)-vinyl]-chromen-2-one (**CS-P**), and its photophysical properties and intracellular pH sensitivity were studied.

### Experimental

#### Materials and methods

All chemicals and solvents were at analytical grade and freshly distilled prior to use without further purification, except

spectrographically pure dimethylsulfoxide (DMSO) used for biological evaluation. Chloroquine was commercially available from Aldrich (St. Louis, MO) and used without further purification. Double distilled water was used for preparation of the buffer solutions.  $^1\text{H}$  NMR and  $^{13}\text{C}$  NMR spectra were measured by BrukerAvance AV II-400 MHz spectrometer. FT-IR spectra were recorded on a Perkin-Elmer 2000 infrared spectrometer with KBr pellets under an ambient atmosphere. UV-Vis absorption spectra were performed on a Perkin Elmer Lambda 950 UV/VIS Spectrometer. Fluorescence spectra were collected on a PerkinElmer LS55 fluorescence spectrophotometer using excitation wavelength of 400 nm. The pH values were determined with PHS-3E pH Meter calibrated at room temperature ( $25 \pm 2^\circ\text{C}$ ) with standard buffers of pH 6.86 and 4.00. Acetic acid and sodium acetate were used for tuning pH values. Fluorescence microscopic images were obtained from High-speed Widefield Live-cell System (Leica AF7000).

### Synthesis

The detailed synthetic routes were shown in Scheme 1. 4-piperidin-1-yl-benzaldehyde<sup>28</sup> and 7-diethylamino-chromen-2-one<sup>29</sup> were synthesized according to the literature procedures.

#### Synthesis of 1-(4-vinyl-phenyl)-piperidine (1)

*n*-BuLi (3.2 mL of 2.5 M in *n*-hexane) was added dropwise to a stirred solution of  $\text{Ph}_3\text{PCH}_2\text{I}$  (3.2 g, 7.85 mmol) in THF (25 mL) at  $0^\circ\text{C}$  under inert atmosphere. After stirring for 30 min, a solution of 4-piperidin-1-yl-benzaldehyde (5.23 mmol) in THF (10 mL) was added dropwise and the resulting mixture was stirred at room temperature for 10 h. Then, saturated ammonium chloride was added and followed by extracting with PE. The organic layer was washed with brine before being dried over anhydrous magnesium sulfate. After evaporating off the solvent, the residue was purified by column chromatography on silica gel to give a pure yellow solid (Yield: 85.0 %).  $^1\text{H}$  NMR (400 MHz,  $\text{CDCl}_3$ )  $\delta$  (ppm): 7.31 (d,  $J = 8.4$  Hz, 2 H, ArH), 6.89 (d,  $J = 8.4$  Hz, 2 H, ArH), 6.67-6.60 (m, 1 H, =CH), 5.58 (d,  $J = 7.2$  Hz, 1 H, =CH<sub>2</sub>), 5.07 (d,  $J = 10.8$  Hz, 1 H, =CH<sub>2</sub>), 3.18 (t,  $J = 5.4$  Hz, 4 H, -CH<sub>2</sub>), 1.73-1.68 (m, 4 H, -CH<sub>2</sub>), 1.61-1.58 (m, 2 H, -CH<sub>2</sub>).

#### Synthesis of 3-bromo-7-diethylamino-chromen-2-one (2)

$\text{Br}_2$  (1.4 g, 9.2 mmol) was added dropwise to a solution of 7-diethylamino-chromen-2-one (2.0 g, 9.2 mmol) in acetic acid (40 mL), and the mixture was stirred at room temperature for 2 h. After completion of the reaction, the precipitate was filtered off and washed with acetic acid, then dried under vacuum and recrystallized in acetonitrile to afford a light yellow solid (Yield: 80.6%).  $^1\text{H}$  NMR (400 MHz,  $\text{DMSO}-d_6$ )  $\delta$  (ppm): 8.34 (s, 1 H, ArH), 7.44 (d,  $J = 8.8$  Hz, 1 H, ArH), 6.75 (dd,  $J = 8.8$  Hz,  $J = 2.4$  Hz, 1 H, ArH), 6.56 (s, 1 H, ArH), 3.45-3.41 (m, 4 H, -CH<sub>2</sub>), 1.13 (t,  $J = 7.2$  Hz, 6 H, -CH<sub>3</sub>).

#### General procedure for the synthesis of target compound

**2** (0.3 g, 1.01 mmol), appropriate styrene (1.1 eq), tris(*o*-tolyl) phosphine (12.28 mg, 0.0404 mmol), palladium acetate (4.52 mg, 0.0202 mmol) and  $\text{Et}_3\text{N}$  (1.97 mL, 14.14 mmol) were added in 24 mL of argon degassed DMF in a flask. After stirring at  $100^\circ\text{C}$  for 24 h under argon, the mixture was cooled to room temperature and poured into water. Resulting solid was filtered off and washed with water, then dried. The crude product residue was purified by column chromatograph over silica to yield the pure product.

#### 7-diethylamino-3-styryl-chromen-2-one (CS)

Orange red solid. Recrystallized from ethanol. Yield: 46.9 %;  $^1\text{H}$  NMR (400 MHz,  $\text{CDCl}_3$ )  $\delta$  (ppm): 7.68 (s, 1 H, ArH), 7.52 (d,  $J = 7.6$  Hz, 2 H, ArH), 7.47 (d,  $J = 16.0$  Hz, 1 H, =CH), 7.36 (t,  $J = 7.2$  Hz, 2 H, ArH), 7.30 (d,  $J = 8.8$  Hz, 1 H, ArH), 7.24 (d,  $J = 7.2$  Hz, 1 H, ArH), 7.11 (d,  $J = 16.0$  Hz, 1 H, =CH), 6.60 (dd,  $J = 8.8$  Hz,  $J = 2.4$  Hz, 1 H, ArH), 6.51 (d,  $J = 2.4$  Hz, 1 H, ArH), 3.45-3.39 (m, 4 H, -CH<sub>2</sub>), 1.23 (t,  $J = 6.8$  Hz, 6 H, -CH<sub>3</sub>).  $^{13}\text{C}$  NMR (100 MHz,  $\text{CDCl}_3$ ):  $\delta$  (ppm) 161.5, 155.6, 150.4, 138.0, 137.6, 130.0, 128.8, 128.7, 127.6, 126.6, 123.1, 117.8, 109.1, 109.0, 97.2, 44.9, 12.5. IR (KBr),  $\text{cm}^{-1}$ : 3070, 3021, 2975, 2920, 1704, 1616, 1587, 1523, 1238, 1139, 975, 750. MS (ESI)<sup>+</sup>:  $m/z$  320.1644 (M + H)<sup>+</sup>; calcd for (M + H)<sup>+</sup>: 320.1651.

#### 7-diethylamino-3-[2-(4-piperidin-1-yl-phenyl)-vinyl]-chromen-2-one (CS-P)

Yellow solid. Yield: 56.1 %;  $^1\text{H}$  NMR (400 MHz,  $\text{CDCl}_3$ )  $\delta$  (ppm): 7.63 (s, 1 H, ArH), 7.42 (d,  $J = 8.4$  Hz, 2 H, ArH), 7.36 (d,  $J = 16.0$  Hz, 1 H, =CH), 7.28 (d,  $J = 8.0$  Hz, 1 H, ArH), 6.97 (d,  $J = 16.0$  Hz, 1 H, =CH), 6.90 (d,  $J = 8.4$  Hz, 2 H, ArH), 6.59 (dd,  $J = 8.8$  Hz,  $J = 2.0$  Hz, 1 H, ArH), 6.51 (d,  $J = 1.6$  Hz, 1 H, ArH), 3.44-3.38 (m, 4 H, -CH<sub>2</sub>), 3.22 (t,  $J = 5.2$  Hz, 4 H, -CH<sub>2</sub>), 1.73-1.67 (m, 4 H, -CH<sub>2</sub>), 1.62-1.57 (m, 2 H, -CH<sub>2</sub>), 1.23 (t,  $J = 7.2$  Hz, 6 H, -CH<sub>3</sub>).  $^{13}\text{C}$  NMR (100 MHz,  $\text{CDCl}_3$ ):  $\delta$  (ppm) 161.7, 155.3, 151.5, 150.0, 136.3, 129.9, 128.5, 128.2, 127.6, 119.6, 118.6, 115.9, 109.3, 109.0, 97.2, 50.1, 44.8, 29.7, 25.7, 24.4, 12.5. IR (KBr),  $\text{cm}^{-1}$ : 2971, 2925, 2849, 1704, 1594, 1511, 1232, 1128, 810. MS (ESI)<sup>+</sup>:  $m/z$  403.2383 (M + H)<sup>+</sup>; calcd for (M + H)<sup>+</sup>: 403.2386.

#### Solvatochromic effects of CS and CS-P

CS, CS-P (8  $\mu\text{M}$ ) were prepared in cyclohexane, toluene, tetrahydrofuran, acetonitrile or dimethyl sulfoxide, respectively. Absorption spectra and fluorescence emission spectra of CS, CS-P in different solvents were recorded ( $\lambda_{\text{ex}} = 400$  nm).

#### Fluorescence changes of CS-P under different pH values

CS and CS-P (4  $\mu\text{M}$ ) were prepared in DMSO-water (1:1, v/v) buffer solution. These solutions were modulated by acetic acid and sodium acetate to achieve different pH values (3.0 ~ 7.6) with maintaining  $\text{Na}^+$  concentration of 0.1 mol/L. After the solutions were kept at ambient temperature for 1-2 h, the fluorescence emission spectra were recorded ( $\lambda_{\text{ex}} = 400$  nm).

The constant  $pK_a$  of CS-P was calculated based on the following formula,  $F_{\text{min}}$  and  $F_{\text{max}}$  represented the fluorescence

intensity at minimal and maximal  $H^+$ , respectively, and  $n$  meant the stoichiometry of  $H^+$  binding to the probe.

$$F = \frac{F_{\max}[H^+]^n + F_{\min}K_a}{K_a + [H^+]^n}$$

In addition, absorption spectra of **CS-P** (4  $\mu$ M) in a DMSO-water solution (1:1, v/v) with different pH values were recorded.

### The selectivity of **CS-P** for $H^+$

Considering that nitrogen and oxygen could bind many metal ions in solution, it was very important to determine whether other ions were potential interferents to **CS-P**. The metal ions and biologically relevant analytes,  $Zn(NO_3)_2$ ,  $MgSO_4$ ,  $NaCl$ ,  $MnSO_4$ ,  $BaCl_2$ ,  $KCl$ ,  $CaCl_2$ ,  $CuSO_4$ ,  $FeCl_3$ ,  $Cr(NO_3)_3$ ,  $FeSO_4$ ,  $NiSO_4$ ,  $HgCl_2$ ,  $Pb(NO_3)_2$ , L-cystine and reduced glutathione, with the same concentration of 40  $\mu$ M, were added as interferents to the solution (DMSO:H<sub>2</sub>O = 1:1, v/v) of **CS-P** (ultimate concentration: 4  $\mu$ M). Fluorescence emission spectra of these solutions were recorded with excitation at 400 nm.

### Tracing intracellular pH changes

Mouse macrophages Raw 264.7 cells were cultured in 24-well plate in this paper and were internalized with 2  $\mu$ M **CS-P** for 15 min at 37 °C, then washed three times with PBS buffer to remove excess probe, chloroquine (100  $\mu$ M) was added to stimulate lysosomal pH change based on the reference.<sup>15</sup> Cells were observed under High-speed Widefield Live-cell System (Leica AF7000) from 0 minute to 60 minute with a time interval of 3 minutes.

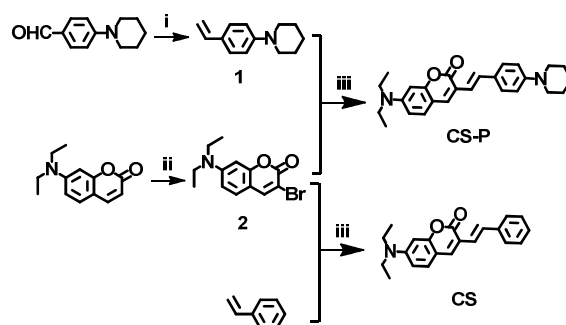
HeLa cells were co-cultured with **CS-P** (2  $\mu$ M) in 24-well plate for 15 min, then washed with fresh DMEM medium and dexamethasone (2  $\mu$ M) was added to decreasing the cellular pH. Cells were observed and recorded by High-speed Widefield Live-cell System (Leica AF7000) from 0 minute to 60 minute with a time interval of 3 minutes.

Furthermore, in order to determine the cellular location of **CS-P**, MG63 cells were co-stained with LysoTracker® Red (0.1  $\mu$ M) (L7528, Invitrogen) or MitoTracker® Deep Red (0.1  $\mu$ M) (M22426, Invitrogen), respectively.

## Results and discussion

### Synthesis

The new coumarin derivative, **CS-P**, was synthesized from 1-(4-vinyl-phenyl)-piperidine and 3-bromo-7-diethylamino-chromen-2-one shown in Scheme 1. Their structures were confirmed by <sup>1</sup>H NMR, <sup>13</sup>C NMR. 7-diethylamino-3-styryl-chromen-2-one (**CS**) was synthesized and used as control to reveal the primary mechanism of fluorescence changes of **CS-P** in the different pH condition, the structure difference between **CS** and **CS-P** was that **CS-P** was constructed by piperidine group on the stem of coumarin. Piperidine derivatives were effective proton receptors with different  $pK_a$  values depending on the skeletons and position of substituents on the piperidine group.<sup>30, 31</sup>



**Scheme 1** The synthetic routes of the objective compounds. (i) BuLi,  $Ph_3PCH_3$ , THF, 0 °C; (ii)  $Br_2$ ,  $CH_3COOH$ ; (iii)  $Pd(OAc)_2$ ,  $P(O-tolyl)_3$ ,  $Et_3N$ , DMF, 100 °C.

### Solvatochromic Effects

Solvatochromism of **CS**, **CS-P** were investigated in several solvents. The photophysical properties of **CS**, **CS-P** were compiled in Table S1. The absorption spectra and the fluorescence emission spectra of **CS** and **CS-P** in various solvents were shown in Figure S1 and Figure S2, respectively. The  $\lambda_{abs}(max)$  and  $\lambda_{em}(max)$  values of **CS-P** were strongly affected by solvent polarity. These results showed that piperidine, the functional group on the **CS-P**, aroused of a bathochromic shift of 25–40 nm, compared with **CS**. A large Stokes shift (>75 nm) and solvent-dependent emission spectra indicated that effective intramolecular charge transfer (ICT) had occurred in the excited state between the coumarin unit and the substituent at position 3.

### Spectral studies of **CS-P**

The absorption spectra, excitation spectra and the fluorescence spectra of **CS-P** at different pH values were shown in Figure S3(A), Figure S3(C) and Figure 1(A), respectively. Along with decreasing of the pH value from 7.6–3.0, the absorbance was significantly enhanced at 443 nm. In the meanwhile, the color of the solution changed from dark yellow to bright yellow-green, which indicated that **CS-P** could serve as a visual indicator for  $H^+$  concentration (Figure S3(B)). Figure 1(A) showed that only very weak fluorescence intensity was observed in pH = 5.9–7.6 solution. However, the fluorescence intensity was significantly enhanced with pH values decreased from pH 5.9 to 3.0. The intensity of **CS-P** in pH 3.0 showed more than 47 fold higher compared with in pH 5.9, while the fluorescent intensity of the control compound, **CS**, did not change in different pH values (Figure S4.). The analysis of emission intensities changed at 515 nm as a function of pH obtained a  $pK_a$  of 4.55 (Figure 1(B)), the  $pK_a$  value almost matched with the typical pH value of the acidic organelles (such as lysosomes and endosomes), which indicated that **CS-P** could be suitable for monitoring pH variations in the acidic environments (pH 4–6) *in vitro*.



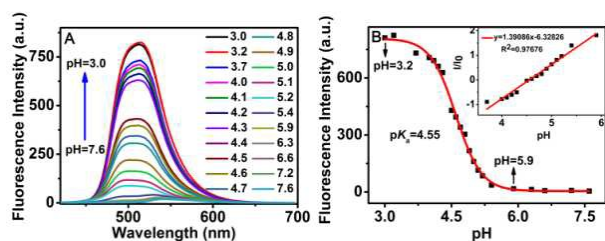


**Figure 1** (A) Fluorescence spectra of **CS-P** (4  $\mu\text{M}$ ) in various pH (7.6-3.0) in DMSO-water (1:1, v/v) solution ( $\lambda_{\text{ex}} = 400 \text{ nm}$ ). (B) Sigmoidal fitting of the pH-dependent fluorescence intensity at 515 nm. Inset: the good linearity in the pH range of 3.2-5.9.

### The switching mechanism

**CS-P** and its protonated form of HCl were prepared to study the proton-binding behavior by  $^1\text{H}$  NMR spectroscopy. As shown in Figure 2(A),  $\text{H}_b$  and  $\text{H}_c$  displayed a slight downfield shift of 0.05 and 0.04 ppm, respectively, suggesting that the diethylamine on the **CS-P** did not bind  $\text{H}^+$ . However  $\text{H}_a$  displayed significant downfield shifts of 0.74 ppm, indicating that the protonation occurred at the piperidine site. The possible mechanism of pH sensitivity of **CS-P** was illustrated in Figure 2(B). Under neutral pH condition (pH = 7.2), **CS-P** existed intramolecular charge transfer (ICT) process from piperidine part to coumarin matrix and weak fluorescence was due to strongly affected by solvent polarity. In contrast, under acidic pH condition (pH = 4.3), the nitrogen atom of piperidine group was protonated, which inhibited the ICT process and led to fluorescence enhancement.

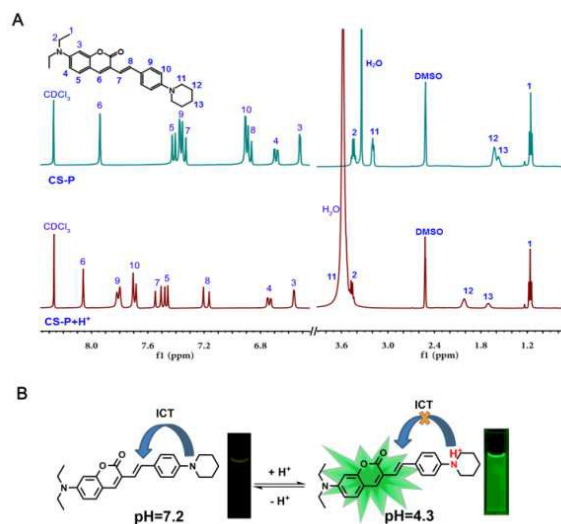


**Figure 2** (A)  $^1\text{H}$  NMR spectra of **CS-P** and **CS-P·HCl** in  $(\text{CD}_3)_2\text{SO}-\text{CDCl}_3$  (4:1, v/v), (B) Mechanism of pH response by protonation and deprotonation of **CS-P**.

### Testing of the selectivity, reversibility and photostability

Considering that nitrogen and oxygen could bind many metal ions in solution, it was very important to determine whether other ions were potential interferents. Upon addition of  $\text{Na}^+$ ,  $\text{K}^+$ ,  $\text{Mg}^{2+}$ ,  $\text{Ca}^{2+}$ ,  $\text{Ba}^{2+}$ ,  $\text{Mn}^{2+}$ ,  $\text{Cr}^{3+}$ ,  $\text{Ni}^{2+}$ ,  $\text{Cu}^{2+}$ ,  $\text{Pb}^{2+}$ ,  $\text{Zn}^{2+}$ ,  $\text{Fe}^{3+}$  and  $\text{Fe}^{2+}$  to the 4  $\mu\text{M}$  **CS-P** solutions while keeping the

experimental condition unchanged at pH 7.2, the results (Figure 3) showed these cations did not increase the fluorescent intensity of **CS-P**. Moreover, amino acids (Cys and GSH) also exhibited negligible effects on the activity of **CS-P**, only a certain amount of  $\text{H}^+$  could lead to remarkable fluorescence enhancement. The competition experiments of **CS-P** revealed that the  $\text{H}^+$ -dependent fluorescence response was unaffected in the presence of background ions (Figure S5). The fluorescent intensity of **CS-P** could be reversibly selected by protonation/deprotonation of the piperidine moiety under acidic or alkaline condition (Figure S6). In addition, it exhibited high photostability (Figure S7). The high selectivity of **CS-P** over interferents, along with its photostability and reversibility, indicated **CS-P** had considerable potential as practical pH probe.

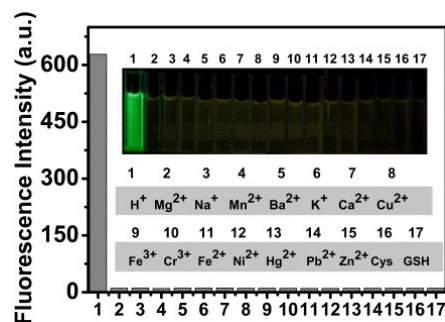


**Figure 3** Fluorescence response (515 nm) of **CS-P** interfered by different ions and amino acids in DMSO-water (1:1, v/v) solution.

### Tracing intracellular pH changes

The cytotoxicity of **CS-P** was evaluated by the MTT assays. **CS-P** showed no cytotoxicity (Figure S8).

*In vitro* cell imaging was carried by employing **CS-P** to monitor intracellular pH changes induced by chloroquine in Raw 264.7 cells. Chloroquine could increase intracellular pH in macrophage cells.<sup>32</sup> **CS-P** exhibited strong yellow fluorescence in these cells before treated with chloroquine, the fluorescence intensities reduced distinctly in the cells by addition of chloroquine according to continuous observation within 60 min (Figure 4).

Dexamethasone could induce cell apoptosis and intracellular acidification was happened spontaneously.<sup>15</sup> After treatment with dexamethasone, the yellow fluorescence intensities in HeLa cells increased gradually which indicated that the intracellular pH (especially these areas adjacent to the cell nuclei) became more and more acidic. Figure 5 showed that the addition of dexamethasone caused apoptosis of HeLa cells and time-dependent increasing of fluorescence intensity, which in accordance with previous report on the apoptosis process and the pH changes in HeLa cells.<sup>26</sup> These results suggested that intracellular acidifications might be possibly due to the release of lysosomal proton in the apoptosis process. The increasing of fluorescence intensity in HeLa cells induced by dexamethasone was coincided with the results observed from RAW264.7 cells induced by chloroquine.

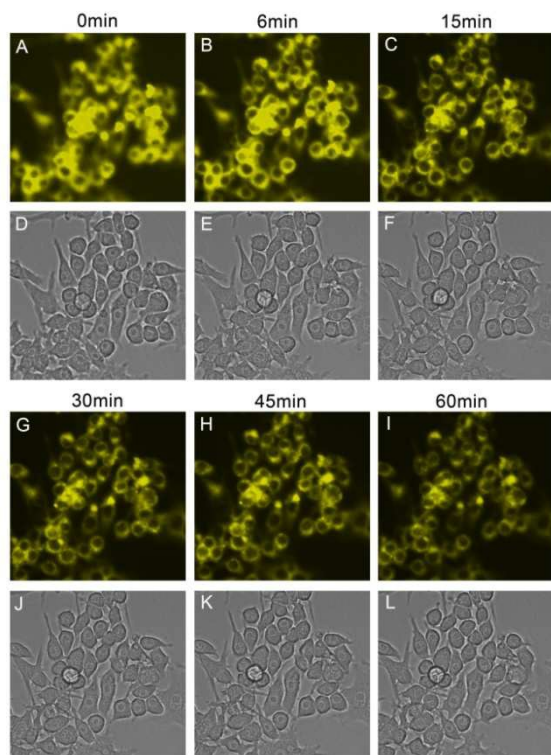


**Figure 4** Fluorescent intensities (yellow) were decreased distinctly along with pH changes induced by chloroquine for mouse macrophage Raw 264.7.

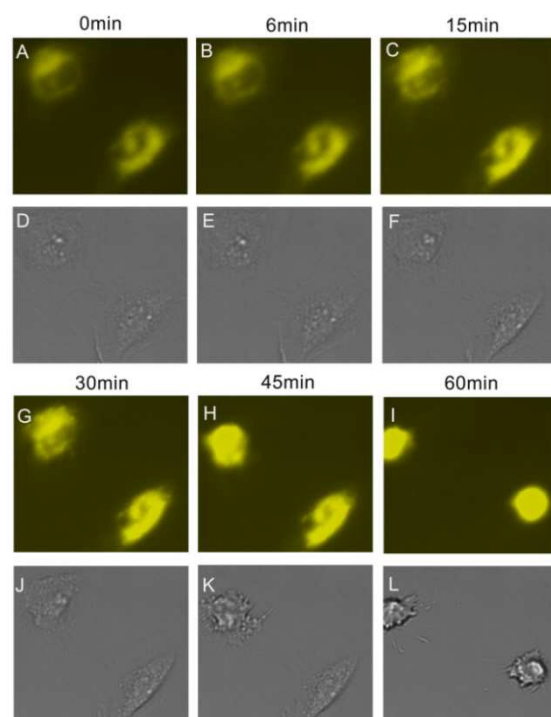


**Figure 5** Fluorescent intensities of CS-P (yellow) were increased gradually along with pH changes in HeLa cells induced by dexamethasone which was caused to apoptosis status.

The pH value of cells would be changed in many cases, such as cancer and Alzheimer's disease,<sup>33</sup> weakly basic

substances can cause the leakage of protons out of lysosomal in the form of protonated bases,<sup>32</sup> while a parts of compounds could decreased the pH value.<sup>15</sup> However it was difficult to determine the intracellular pH changes in a single cell. **CS-P** proved a potential way to realize the detection of the cell pH changes.

**CS-P** showed high pH sensitive ranged from pH 5.9 to pH 3.0, which was suitable for tracing the intracellular pH changes. Furthermore, in order to determine the intracellular organelle distribution of **CS-P** (2  $\mu$ M), we co-stained the MG63 cells with LysoTracker® Red (0.1  $\mu$ M) (L7528, Invitrogen) or MitoTracker® Deep Red, respectively. The results were shown in Figure 6, the yellow fluorescence was observed in cytoplasm (Figure 6A and 6D), but in the merged figure the **CS-P** did not existed in lysosome (Figure 6C) or mitochondria (Figure 6F). These results proved that **CS-P** was localized in cytoplasm.

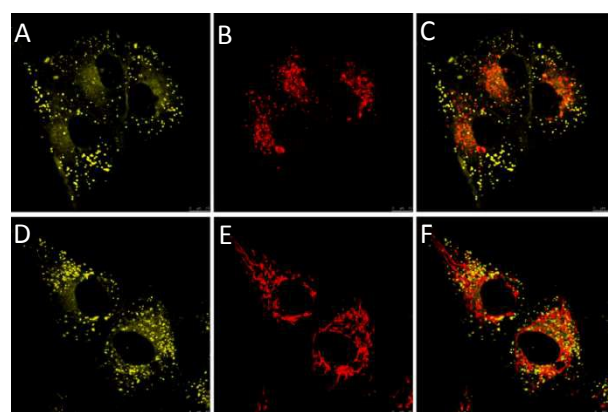


**Figure 6** Cellular Location experiment of **CS-P**. (A, D): Yellow emission for **CS-P**; (B) Red emission for LysoTracker® Red; (E) MitoTracker® Deep Red. (C) Merged A and B. (F) Merged C and D.

## Conclusions

In summary, a new coumarin derivative as pH sensitive probe was designed and synthesized. **CS-P** exhibited high pH sensitive ranged from pH 5.9 to pH 3.0 and its  $pK_a = 4.55$ . *In vitro* cell culture results showed that the fluorescence intensity of **CS-P** could indicate the cellular pH changes distinctly. Furthermore, **CS-P** was localized in cytoplasm after entered in cells. These preliminary works demonstrated that **CS-P** was a promising candidate for tracing cellular pH changes.

## Acknowledgements

The authors acknowledge the financial support for this work by Research Fund for the Doctoral Program of Higher Education of China (20130181110089), the National Natural Science Foundation of China (NSFC) (Grants No. 21372168) and National Key Technology R&D Program (2012BAI42G01). Electronic Supplementary Information (ESI) available: [details of any supplementary information available should be included here]. See DOI: 10.1039/c000000x/

## Notes and references

<sup>a</sup>Key Laboratory of Green Chemistry and Technology (Ministry of Education), College of Chemistry, Sichuan University, Chengdu 610064, China.

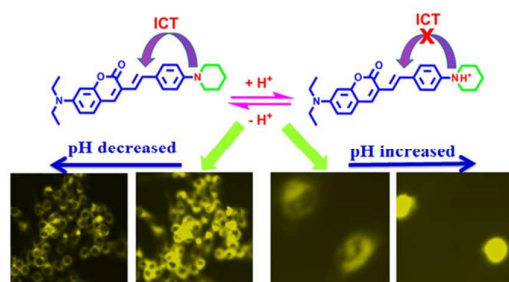
<sup>b</sup>National Engineering Research Center for Biomaterials, Sichuan University, Chengdu, 610064, China.

<sup>c</sup>Department of Biochemistry and Molecular Biology, West China School of Preclinical and Forensic Medicine, Sichuan University, Chengdu, 610041, China.

\*These two authors contributed equally to this work.

email : tanyf@scu.edu.cn (Y. Tan); jiangq@scu.edu.cn (Q. Jiang)

- 1 N. Grandin, M. Charbonneau, *J Cell Sci*, 1991, **99**, 5.
- 2 S. Matsuyama, J. C. Reed, *Cell Death Differ*, 2000, **7**, 1155.
- 3 D.G. Nicholls, I. D. Scott, *Biochem J*, 1980, **186**, 833.
- 4 H. Karaki, S. Kitajima, H. Ozaki, *Nihon Rinsho Jpn J Clin Med*, 1992, **50**, 2106.
- 5 A. J. Jannecki, M. H. Montrose, P. Zimniak, A. Zweibaum, C. M. Tse, S. Khurana, *J Biol Chem*, 1998, **273**, 8790.
- 6 E. De Candia, G. A. Lanza, E. Romagnoli, G. Ciabattini, A. Sestito, P. Pasqualetti, *Int J Cardiol*, 2005, **100**, 371.
- 7 A. Kogot-Levin, M. Zeigler, A. Ornoy, G. Bach, *Pediatr Res*, 2009, **65**, 686.
- 8 I. N. Rich, I. Brackmann, D. Worthington-White, M. J. Dewey. *J Cell Physiol*, 1998, **177**, 109.
- 9 J. R. Casey, S. Grinstein, J. Orłowski, *Nat Rev Mol Cell Bio*, 2010, **11**, 50.
- 10 J. Han, K. Burgess, *Chem Rev*, 2010, **110**, 2709.
- 11 L. Yuan, W. Y. Lin, L. Tan, K. B. Zheng, W. M. Huang, *Angew Chem Int Ed*, 2013, **52**, 1628.
- 12 Y. M. Xiang, B. Y. He, X. F. Li, Q. Zhu, *Rsc Adv*, 2013, **3**, 4876.
- 13 K. M. Wang, J. Huang, X. H. Yang, X. X. He, J. B. Liu, *Analyst*, 2013, **138**, 62.
- 14 T. Terai, T. Nagano, *Pflug Arch Eur J Phy*, 2013, **465**, 347.
- 15 H. Zhu, J. Fan, Q. Xu, H. Li, J. Wang, P. Gao, *Chem Commun*, 2012, **48**, 11766.
- 16 J. Han, A. Loudet, R. Barhoumi, R. C. Burghardt, K. Burgess, *J Am Chem Soc*, 2009, **131**, 1642.
- 17 Y. H. Chan, C. Wu, F. Ye, Y. Jin, P. B. Smith, D. T. Chiu, *Anal Chem*, 2011, **83**, 1448.
- 18 T. Myochin, K. Kiyose, K. Hanaoka, H. Kojima, T. Terai, T. Nagano, *J Am Chem Soc*, 2011, **133**, 3401.
- 19 (a) R. Sun, W. Liu, Y. J. Xu, J. M. Lu, J. F. Ge, M. Ihara, *Chem. Commun.* 2013, **49**, 10709; (b) W. Liu, R. Sun, J. F. Ge, Y. J. Xu, Y. Xu, J. M. Lu, I. Itoh, M. Ihara, *Anal Chem*, 2013, **85**, 7419.
- 20 M. Lee, N. G. Gubernator, D. Sulzer, D. Sames, *J Am Chem Soc*, 2010, **132**, 8828.
- 21 E. Herz, T. Marchincin, L. Connelly, D. Bonner, A. Burns, S. Switalski, *J Fluoresc*, 2010, **20**, 67.
- 22 H. E. Katerinopoulos, *Curr Pharm Design*, 2004, **10**, 3835.
- 23 A. O. Uwaifo, *J Toxicol Env Heal*, 1984, **13**, 521.
- 24 S. S. Zhu, W. Y. Lin, L. Yuan, *Dyes Pigm*, 2013, **99**, 465.
- 25 H. S. Peng, J. A. Stolwijk, L. N. Sun, J. Wegener, O. S. Wolfbeis, *Angew Chem Int Ed*, 2010, **49**, 4246.
- 26 X. F. Zhou, F. Y. Su, H. G. Lu, P. Senechal-Willis, Y. Q. Tian, R. H. Johnson, *Biomaterials*, 2012, **33**, 171.
- 27 X. D. Liu, Y. Xu, R. Sun, Y. J. Xu, J. M. Lu, J. F. Ge, *Analyst*, 2013, **138**, 6542.
- 28 P. Magdolen, M. Meciarova, S. Toma, *Tetrahedron*, 2001, **57**, 4781.
- 29 D. Ray, P. K. Bharadwaj, *Inorg Chem*, 2008, **47**, 2252.
- 30 X. P. Chen, J. S. Jin, N. N. Wang, P. Lu, Y. G. Wang, *Eur J Org Chem*, 2012, 824.
- 31 A. K. Leslie, D. D. Li, K. Koide, *J Org Chem*, 2011, **76**, 6860.
- 32 B. Poole, S. Ohkuma, *J Cell Biol*, 1981, **90**, 665.
- 33 D. Ibarreta, E. Urcelay, R. Parrilla, M. S. Ayuso, *Ann Neurol*, 1998, **44**, 216.



A novel coumarin derivative was synthesized and its application in live cell imaging was demonstrated.